

# Absence of spin current generation in Ti/FeCoB bilayers with strong interfacial spin-orbit coupling

Lijun Zhu\*, Robert A. Buhrman  
 Cornell University, Ithaca, New York 14850, USA  
 \*lz442@cornell.edu

We report a quantitative investigation of the absence/presence of spin current generation by interfacial spin-orbit coupling (ISOC) at a normal metal/ferromagnet (NM/FM) interface. Utilizing the Ti/FeCoB bilayers which are unique for the negligible spin Hall effect and strong tunable ISOC, we establish direct experimental evidence that there is no significant spin current generation at NM/FM interface via spin-orbit filtering effect or Rashba-Edelstein effect even when the ISOC is stronger than that of a typical Pt/FM interface and can promote strong perpendicular magnetic anisotropy. This result also suggests that  $3d$  Ti has minimal orbital Hall effect.

Generation of spin current has been the focus of spintronics that aims at the development of energy-efficient and high-speed manipulation of magnetic memory [1-5] and logic [6]. Spin current can be generated by the spin Hall effect (SHE)[1,7,8], the topological surface states [9,10], the anomalous Hall effect [11,12], the planar Hall effect [13,14], spin Seebeck effect [15], spin pumping [16], or non-centrosymmetric crystals [17]. Recently, interfacial spin-orbit coupling (ISOC) of a normal metal/ferromagnet (NM/FM) interface was also proposed to generate non-local spin current and thus dampinglike spin-orbit torque (SOT)[18-22]. First, in the spin-orbit filtering effect [20], the un-polarized current in the NM is selectively scattered by a strong ISOC of the NM/FM interface so that the transmitted current becomes transversely spin polarized and exerts a dampinglike SOT on the adjacent FM layer (Fig. 1). Moreover, the Rashba-Edelstein effect may generate spin current and dampinglike SOT only if carriers were scattered across the NM/FM interface [18-20]. In addition, orbital current generated by the orbital Hall effect of a NM can be converted into spin current via spin-orbit coupling (SOC) of an interface or a FM [21,22]. While these theoretical proposals have significantly enriched the physical understanding, both the amplitude and the polarization direction of interface-generated spin currents, if any, are challenging to identify in most heavy metal/FM heterostructures [23-25] because of spin current generation by the SHE and spin memory loss by ISOC [26-28].

In this work, we quantitatively investigate the potential effects of ISOC in Ti/FeCoB bilayers that are unique because of the minimal SHE, the negligible bulk SOC in Ti, and a tunable ISOC at the same time. By varying the Ti thickness ( $d$ ), the strength of the ISOC at Ti/FeCoB interface is tuned from negligibly small to greater than that of typical Pt/FeCoB and Pt/Co interfaces. From this ability, we find that both dampinglike and fieldlike SOTs in the Ti/FeCoB bilayers are minimal regardless of  $d$  and the ISOC strength, indicating no significant spin current generation by the spin-orbit filtering effect, the Rashba-Edelstein effect, or orbit-spin conversion.

We sputter-deposited perpendicularly magnetized bilayers of Ti 1.5-7/FeCoB 1 (the numbers are layer thickness in nm; FeCoB = Fe<sub>0.6</sub>Co<sub>0.2</sub>B<sub>0.2</sub>) and in-plane magnetized Ti 1.5-7/FeCoB 2 onto oxidized Si substrates. Each sample is capped with a 2 nm MgO and a 1.5 nm Ta layer that is oxidized upon exposure to air (see the cross-sectional scanning transmission electron microscopy and electron energy loss spectrum results in [29]). Each sample was

patterned into  $5 \times 60 \mu\text{m}^2$  Hall bars for measuring the SOTs and the ISOC by harmonic Hall voltage response (HHVR) measurements [30-32].

According to Bruno's model [33,34], the interfacial perpendicular magnetic anisotropy (PMA) energy density ( $K_s^{\text{ISOC}}$ ) of a NM/FM interface is determined by the ISOC and interfacial orbital hybridization, i.e.  $K_s^{\text{ISOC}}/t_{\text{FM}} \propto \zeta (m_0^\perp - m_0^\parallel)$ , where  $t_{\text{FM}}$ ,  $m_0^\perp$ ,  $m_0^\parallel$  are the thickness, the perpendicular orbital magnetic moment, and the in-plane orbital magnetic moment of the FM layer, and  $\zeta$  is the ISOC energy of the interface, respectively. It has also been well established that  $m_0^\perp$  is localized at the first atomic layer of the FM adjacent to the interface [33,34], i.e.  $m_0^\perp = m_{0,i}^\perp/t_{\text{FM}} + m_0^\parallel$ , where  $m_{0,i}^\perp$  is the  $m_0^\perp$  value for the single FM interface layer and  $m_0^\parallel$  is thickness-insensitive and reasonably approximates the bulk orbital magnetic moment value for the FM [34,35]. As a result,  $K_s^{\text{ISOC}} \propto \zeta m_{0,i}^\perp$  for the NM/FM interfaces. It has also been established that the Rashba constant ( $\alpha_R$ ) follows  $\alpha_R \propto \zeta m_{0,i}^\perp/m_0^\parallel$  [36]. Provided that  $m_{0,i}^\perp$  and  $m_0^\parallel$  are approximately invariant with the layer thicknesses [34,35],  $K_s^{\text{ISOC}}$  can be a linear indicator of  $\alpha_R$  of Ti/FeCoB interface.

To quantify  $K_s^{\text{ISOC}}$  for the Ti/FeCoB interface, we first determined the total interfacial PMA energy density ( $K_s$ ) of the two Co interfaces of the Ti/FeCoB/MgO samples using the relation  $H_k \approx -4\pi M_s + 2K_s/M_{s\text{FeCoB}}$ , where  $M_s \approx 1260 \text{ emu/cm}^3$  is the saturation magnetization and  $H_k$  is the effective perpendicular magnetic anisotropy field. The  $H_k$  values for the PMA samples (Fig. 1(b)) are determined by fitting the in-plane field,  $H_x$ , dependence of the in-phase first HHVR ( $V_{1\omega}$ ) to the sinusoidal electric field  $E = 66.7 \text{ kV/cm}$  applied to the Hall bar following the relation

$$V_{1\omega} = \pm V_{\text{AH}} \approx \pm V_{\text{AH}} (1 - H_x^2/2H_k^2), \quad (1)$$

where  $V_{\text{AH}}$  is the anomalous Hall voltage determined by measuring  $V_{1\omega}$  as a function of  $H_z$  (see Fig. 2(a)),  $\theta \approx H/H_k \ll 1$  is the polar angle of the magnetic moment tilted away from the film normal direction, and the signs  $\pm$  correspond to the initial magnetization states of  $\pm M_z$ , respectively. Here, the charge current flows in the  $x$  direction, and  $z$  is the out-of-plane direction. We measured  $H_x$  dependency of  $V_{1\omega}$  for both the  $\pm M_z$  cases (see Fig. 2(b)) and averaged the two values of  $H_k$  for the PMA Ti/FeCoB samples. For the in-plane samples,  $dV_{1\omega}/dH_z$  is first determined under different in-plane bias fields  $H_x$  (Fig. 2(c)),  $H_k$  and  $V_{\text{AH}}$  were then estimated by fitting the data to the relation

$$dV_{1\omega}/dH_z = V_{\text{AH}}/(-H_k + |H_x|). \quad (2)$$

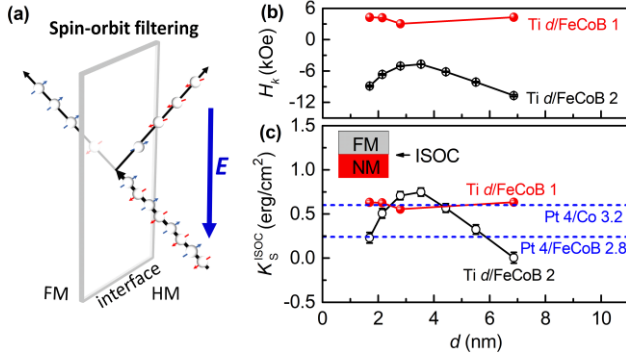


Fig. 1. (a) Schematic depict for the spin-orbit filtering. (b) Perpendicular magnetic anisotropy field ( $H_k$ ) and (c) Interfacial magnetic anisotropy energy density for the Ti/FeCoB interface ( $K_s^{\text{ISOC}}$ ) plotted as a function of the Ti thickness. The two dashed blue lines indicate the  $K_s^{\text{ISOC}}$  values of in-plane magnetized Pt 4/Co 3.2 [37] and Pt 4/FeCoB 2.8 [27], respectively.

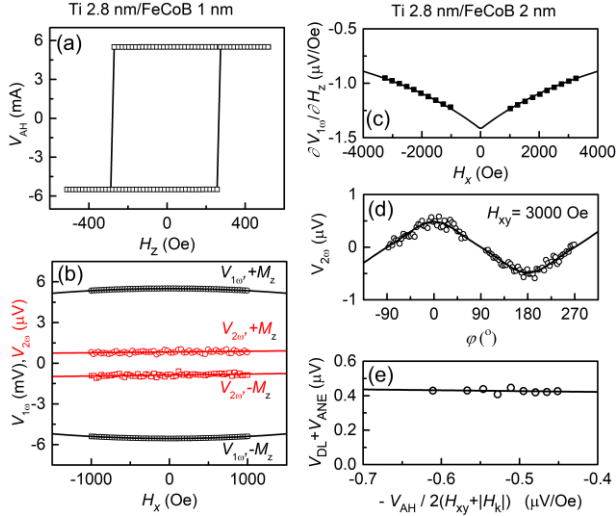


Fig. 2. (a)  $V_{\text{AH}}$  vs  $H_z$  and (b)  $V_{1\omega}$  and  $V_{2\omega}$  vs  $H_x$  for the perpendicularly magnetized Ti 2.8/FeCoB 1. (c)  $\partial V_{1\omega}/\partial H_x$  vs  $H_x$ , (d)  $V_{2\omega}$  vs  $\varphi$  ( $H_{xy} = 3000$  Oe), and (e)  $V_{\text{DL}} + V_{\text{ANE}}$  vs  $-V_{\text{AH}}/2(H_{xy} + |H_k|)$  for the in-plane magnetized Ti 2.8/FeCoB 2. In (b) the red straight lines represent the best linear fits, and the black parabolic lines denote the fits of the data to Eq. (1). In (c), the black curve is the best fit of data to Eq. (2). In (d) the lines represent the best fits of data to Eq. (5). The straight line in (e) represents the best linear fit.

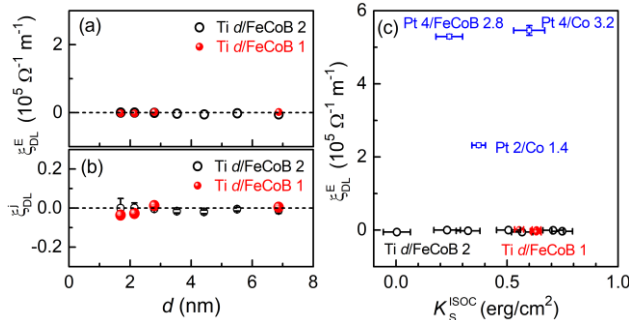


Fig. 3. (a)  $\xi_{\text{DL}}^E$  vs  $d$ , (b)  $\xi_{\text{DL}}^j$  vs  $d$ , and (c)  $\xi_{\text{DL}}^E$  vs  $K_s^{\text{ISOC}}$  for Ti/FeCoB bilayers. The data for the Pt 4/FeCoB 2.8 [37], Pt 4/Co 3.2 [27], and Pt 2/Co 1.4 are plotted in (c) for comparison.

Using  $K_s^{\text{FeCoB/MgO}} \approx 0.6$  erg/cm<sup>2</sup> as determined from a control sample of MgO/FeCoB/MgO, we estimate  $K_s^{\text{ISOC}} = K_s - K_s^{\text{FeCoB/MgO}}$  for the Ti/FeCoB interfaces in Fig. 1(c). For the in-plane magnetized Ti/FeCoB samples,  $K_s^{\text{ISOC}}$  first increases from  $\approx 0.23$  erg/cm<sup>2</sup> at  $d = 1.7$  nm to  $\approx 0.75$  erg/cm<sup>2</sup> at  $d = 3.5$  nm, and then gradually drops to  $\approx 0$  erg/cm<sup>2</sup> at  $d = 6.9$  nm, suggesting a strong tuning of the ISOC strength by the thickness of the Ti layer. In contrast,  $K_s^{\text{ISOC}}$  of the PMA Ti/FeCoB samples (red dots) remains at a high value of  $\approx 0.6$  erg/cm<sup>2</sup>. As indicated by the blue lines in Fig. 1(c),  $K_s^{\text{ISOC}}$  is  $\approx 0.6$  erg/cm<sup>2</sup> for a typical Pt/Co interface [27] and  $\approx 0.24$  erg/cm<sup>2</sup> for a typical Pt/FeCoB interface [37].

The dampinglike (fieldlike) SOT efficiencies per applied electric field,  $\xi_{\text{DL(FL)}}^E$ , and per unit bias current density,  $\xi_{\text{DL(FL)}}^j$ , of the Ti/FeCoB bilayers can be determined using HHVR measurements as [38]

$$\xi_{\text{DL(FL)}}^E = (2e/\hbar) \mu_0 M_s t_{\text{FM}} H_{\text{DL(FL)}}/E. \quad (3)$$

$$\xi_{\text{DL(FL)}}^j = (2e/\hbar) \mu_0 M_s t_{\text{FM}} H_{\text{DL(FL)}}/j. \quad (4)$$

where  $H_{\text{DL(FL)}}$  is the dampinglike (fieldlike) effective SOT field, and  $j$  the bias current density. For Ti 1.5-7/FeCoB 1 with PMA,  $H_{\text{DL(FL)}} = -2 \frac{\partial V_{2\omega}}{\partial H_x(y)} / \frac{\partial^2 V_{1\omega}}{\partial^2 H_x(y)}$  [30], where the in-phase first

HHVR ( $V_{1\omega}$ ) and the out-of-phase second HHVR ( $V_{2\omega}$ ) are parabolic and linear functions of in-plane magnetic fields  $H_x(y)$  [Fig. 2(b)], respectively. Here, we do not apply the so-called ‘‘planar Hall correction’’ in analyzing the out-of-plane HHVR results for the reasons discussed in detail in the Supplementary Materials of Refs. [31] and [39]. For the in-plane magnetized Ti 1.5-7/FeCoB 2,  $H_{\text{DL(FL)}}$  is determined from the angle-dependent HHVR measurements. As shown in Fig. 2(d),  $V_{2\omega}$  follows [32,39]

$$V_{2\omega} = (V_{\text{DL}} + V_{\text{ANE}}) \cos\varphi + V_{\text{FL}} \cos\varphi \cos 2\varphi, \quad (5)$$

where  $V_{\text{DL}} = -V_{\text{AH}} H_{\text{DL}}/2(H_{xy} + |H_k|)$  is the second HHVR to the dampinglike SOT,  $V_{\text{FL}} = V_{\text{PH}} (H_{\text{FL}} + H_{\text{Oe}})/H_{xy}$  the second HHVR to the fieldlike SOT and Oersted field torque,  $V_{\text{ANE}}$  the anomalous Nernst voltage,  $H_{xy}$  the in-plane bias field,  $\varphi$  the in-plane angle of  $H_{xy}$  and thus the magnetization with respect to the current direction.  $H_{\text{DL}}$  and  $H_{\text{FL}}$  are determined from the slope of the linear fit of  $V_{\text{DL}}$  vs  $-V_{\text{AH}}/2(H_{xy} + |H_k|)$  [see Fig. 2(e)] and  $V_{\text{FL}}$  vs  $V_{\text{PH}}/H_{xy}$ , respectively.

As summarized in Fig. 3(a), the obtained values of  $\xi_{\text{DL}}^E$  of the Ti/FeCoB samples are negligibly small regardless of the Ti thickness, i.e.  $|\xi_{\text{DL}}^E| < 0.05 \times 10^5 \Omega^{-1} \text{m}^{-1}$  for Ti/FeCoB in sharp contrast to  $\approx 5.5 \times 10^5 \Omega^{-1} \text{m}^{-1}$  for Pt 4/FeCoB [37] and Pt 4/Co bilayers [27]. The corresponding values of  $\xi_{\text{DL}}^j = \xi_{\text{DL}}^E \rho_{xx}$  are also very small ( $|\xi_{\text{DL}}^j| < 0.025$ ) despite the high resistivity ( $\rho_{xx}$ ) of the thin Ti layer ( $\rho_{xx}$  decreases gradually from 1320  $\mu\Omega$  cm for  $d = 1.7$  nm to 220  $\mu\Omega$  cm for  $d = 6.9$  nm). This first indicates minimal spin current generation due to the SHE and the OHE in Ti. The absence of the so-called ‘‘orbital torque’’ is most likely due to a minimal OHE inside the Ti layer since recent theories and experiments have suggested that the generated orbital current, if any, can be converted to spin current at an interface or inside a FM with strong SOC [21,22].

More importantly, the observed irrelevance of the torque efficiencies to the ISOC strength of the Ti/FeCoB interface (Fig. 3(c)) provide unambiguous evidence that there is no significant interfacial generation of spin current by Rashba-Edelstein effect and spin-orbit filtering in these samples. Note that the spin current generation and thus dampinglike SOT due to an interfacial Rashba-Edelstein or spin filtering effect, if any, should increase linearly with  $\alpha_R$  [19,20] and thus  $K_s^{\text{ISOC}}$ . This result most likely indicates that the interfacial generation of spin current and spin-orbit torques by Rashba-Edelstein effect and spin filtering effect should be also absent in the Pt/Co and the Pt/FeCoB samples and other NM/FM heterostructures which have similar or lower ISOC strength as these Ti/FeCoB interfaces. Instead, the very strong dampinglike SOTs of  $\sim 10^5 \Omega^{-1} \text{m}^{-1}$  in the Pt 4/FeCoB 2.8 [37], Pt 4/Co 3.2 [27], and Pt 2/Co 1.4 in Fig. 3(c) should be entirely attributed to the giant intrinsic SHE of the Pt [7,23,24]. This conclusion is only consistent with the theories that ISOC has negligible contribution to the dampinglike SOT via the “two-dimensional” Rashba-Edelstein effect at HM/FM interfaces [40–43]. This conclusion is also supported by our recent experiments that the dampinglike SOT of  $\text{Au}_{1-x}\text{Pt}_x/\text{Co}$  bilayers varies distinctly different from  $K_s^{\text{ISOC}}$  as a function of the  $\text{Au}_{1-x}\text{Pt}_x$  composition [44] and that the ISOC at HM/FM interfaces acts as the dominant mechanism of spin memory loss [27]. Finally, we mention that the fieldlike torque is also very small,  $\xi_{\text{FL}}^E \approx 0.1 \times 10^5 \Omega^{-1} \text{m}^{-1}$  (see Fig. S1) and shows no obvious correlation to  $K_s^{\text{ISOC}}$  and  $\alpha_R$ .

In summary, we have quantitatively examined the absence/presence of interfacial spin current generation in the Ti/FeCoB bilayers. By varying the layer thicknesses, the strength of the ISOC at Ti/FeCoB interface is tuned from being negligibly small to being greater than that of typical Pt/FeCoB and Pt/Co interfaces. From this ability, we find that both dampinglike and fieldlike SOTs in the Ti/FeCoB bilayers remain minimal regardless of the Ti thickness, the ISOC strength, and the type of magnetic anisotropy. This result most likely suggests the absence of any significant spin current generation by spin-orbit filtering effect and the Rashba-Edelstein effect at the NM/FM interfaces. This result also indicates a negligible SHE and orbital Hall effect in Ti. Our findings should benefit the understanding of spin current generation at NM/FM interfaces.

This work was supported in part by the Office of Naval Research (N00014-15-1-2449), in part by the NSF MRSEC program (DMR-1719875) through the Cornell Center for Materials Research, and in part by the Defense Advanced Research Projects Agency (USDI D18AC00009). The devices were fabricated at the Cornell NanoScale Facility, an NNCI member supported by NSF Grant ECCS-1542081.

[1] L. Liu, C.-F. Pai, Y. Li, H. W. Tseng, D. C. Ralph, R. A. Buhrman, Spin-torque switching with the giant spin Hall effect of tantalum, *Science* 336, 555 (2012).  
 [2] E. Grimaldi, V. Krizakova, G. Sala, F. Yasin, S. Couet, G. S. Kar, K. Garello, P. Gambardella, Single-shot dynamics of spin-orbit torque and spin transfer torque switching in

three-terminal magnetic tunnel junctions, *Nat. Nanotech.* 15, 111–117 (2020).  
 [3] M. Wang, W. Cai, D. Zhu, Z. Wang, J. Kan, Z. Zhao, K. Cao, Z. Wang, Y. Zhang, T. Zhang, C. Park, J.-P. Wang, A. Fert, and W. Zhao, Field-free switching of a perpendicular magnetic tunnel junction through the interplay of spin-orbit and spin-transfer torques, *Nat. Electron.* 1, 582 (2018).  
 [4] S. Fukami, T. Anekawa, C. Zhang, H. Ohno, A spin-orbit torque switching scheme with collinear magnetic easy axis and current configuration, *Nat. Nanotechnol.* 11, 621–625 (2016).  
 [5] L. Zhu, L. Zhu, S. Shi, D. C. Ralph, R. A. Buhrman, Energy-efficient ultrafast SOT-MRAMs based on low-resistivity spin Hall metal  $\text{Au}_{0.25}\text{Pt}_{0.75}$ , *Adv. Electron. Mater.* 6, 1901131 (2020).  
 [6] Z. Luo, et al., Current-driven magnetic domain-wall logic, *Nature* 579, 214–218 (2020).  
 [7] L. Zhu, L. Zhu, M. Sui, D. C. Ralph, R. A. Buhrman, Variation of the giant intrinsic spin Hall conductivity of Pt with carrier lifetime, *Sci. Adv.* 5, eaav8025 (2019).  
 [8] Z. Chi, Y.-C. Lau, X. Xu, T. Ohkubo, K. Hono, M. Hayashi, The spin Hall effect of Bi-Sb alloys driven by thermally excited Dirac-like electrons, *Sci. Adv.* 6, eaay2324 (2020).  
 [9] A. R. Mellnik, J. S. Lee, A. Richardella, J. L. Grab, P. J. Mintun, M. H. Fischer, A. Vaezi, A. Manchon, E.-A. Kim, N. Samarth, D. C. Ralph, Spin-transfer torque generated by a topological insulator, *Nature* 511, 449–451 (2014).  
 [10] Y. Fan, P. Upadhyaya, X. Kou, M. Lang, S. Takei, Z. Wang, J. Tang, L. He, L.-T. Chang, M. Montazeri, G. Yu, W. Jiang, T. Nie, R. N. Schwartz, Y. Tserkovnyak, K. L. Wang, Magnetization switching through giant spin-orbit torque in a magnetically doped topological insulator heterostructure, *Nat. Mater.* 13, 699–704 (2014).  
 [11] T. Taniguchi, J. Grollier, M. D. Stiles, Spin-Transfer Torque Generated by the Anomalous Hall effect and Anisotropic Magnetoresistance, *Phys. Rev. Appl.* 3, 044001 (2015).  
 [12] J. D. Gibbons, D. MacNeill, R. A. Buhrman, and D. C. Ralph, Reorientable Spin Direction for Spin Current Produced by the Anomalous Hall Effect, *Phys. Rev. Applied* 9, 064033 (2018).  
 [13] C. Safranski, E. A. Montoya, I. N. Krivorotov, Spin-orbit torque driven by a planar Hall current, *Nat. Nanotech.* 14, 27–30 (2019).  
 [14] C. Safranski, J. Z. Sun, J.-W. Xu, and A. D. Kent, Planar Hall Driven Torque in a Ferromagnet/Nonmagnet/Ferromagnet System, *Phys. Rev. Lett.* 124, 197204 (2020).  
 [15] K. Uchida, S. Takahashi, K. Harii, J. Ieda, W. Koshibae, K. Ando, S. Maekawa, E. Saitoh, Observation of the spin Seebeck effect, *Nature* 455, 778–781 (2008).  
 [16] Y. Tserkovnyak, A. Brataas, G. E. W. Bauer, Spin pumping and magnetization dynamics in metallic multilayers, *Phys. Rev. B* 66, 224403 (2002).  
 [17] H. Kurebayashi *et al.*, An antidamping spin-orbit torque originating from the Berry curvature, *Nat. Nanotech.* 9, 211–217 (2014).

- [18] V. P. Amin, J. Zemen, M. D. Stiles, Interface-Generated Spin Currents, *Phys. Rev. Lett.* 121, 136805 (2018).
- [19] L. Wang, R. J. H. Wesselink, Y. Liu, Z. Yuan, K. Xia, P. J. Kelly, Giant Room Temperature Interface Spin Hall and Inverse Spin Hall Effects, *Phys. Rev. Lett.* 116, 196602 (2016).
- [20] K.-W. Kim, K.-J. Lee, J. Sinova, H.-W. Lee, M. D. Stiles, Spin-orbit torques from interfacial spin-orbit coupling for various interfaces, *Phys. Rev. B* 96, 104438 (2016).
- [21] D. Go, H.-W. Lee, Orbital torque: Torque generation by orbital current injection, *Phys. Rev. Research* 2, 013177 (2020).
- [22] S. Ding, A. Ross, D. Go, Z. Ren, F. Freimuth, S. Becker, F. Kammerbauer, J. Yang, G. Jakob, Y. Mokrousov, M. Kläui, Harnessing non-local orbital-to-spin conversion of interfacial orbital currents for efficient spin-orbit torque, *Phys. Rev. Lett.* 125, 177201 (2020).
- [23] E. Sagasta, Y. Omori, M. Isasa, M. Gradhand, L. E. Hueso, Y. Niimi, Y. Otani, and F. Casanova, Tuning the spin Hall effect of Pt from the moderately dirty to the superclean regime, *Phys. Rev. B* 94, 060412(R)(2016).
- [24] L. Zhu, R. A. Buhrman, Maximizing spin-orbit torque efficiency of Pt/Ti multilayers: Tradeoff between the intrinsic spin Hall conductivity and carrier lifetime, *Phys. Rev. Appl.* 12, 051002 (2019).
- [25] C. Zhang, S. Fukami, K. Watanabe, A. Ohkawara, S. DuttaGupta, H. Sato, F. Matsukura, H. Ohno, Critical role of W deposition condition on spin-orbit torque induced magnetization switching in nanoscale W/CoFeB/MgO, *Appl. Phys. Lett.* 109, 192405 (2016).
- [26] K. Chen and S. Zhang, Spin Pumping in the Presence of Spin-Orbit Coupling, *Phys. Rev. Lett.* 114, 126602 (2015).
- [27] L. Zhu, D. C. Ralph, and R. A. Buhrman, Spin-Orbit Torques in Heavy-Metal-Ferromagnet Bilayers with Varying Strengths of Interfacial Spin-Orbit Coupling, *Phys. Rev. Lett.* 122, 077201 (2019).
- [28] J.-C. Rojas-Sánchez, N. Reyren, P. Laczkowski, W. Saverio, J.-P. Attané, C. Deranlot, M. Jamet, J.-M. George, L. Vila, and H. Jaffrès, Spin Pumping and Inverse Spin Hall Effect in Platinum: The Essential Role of Spin-Memory Loss at Metallic Interfaces, *Phys. Rev. Lett.* 112, 106602 (2014).
- [29] L. Zhu, X. S. Zhang, D. A. Muller, D. C. Ralph, R. A. Buhrman, Observation of Strong Bulk Damping-Like Spin-Orbit Torque in Chemically Disordered Ferromagnetic Single Layers, *Adv. Funct. Mater.* DOI:10.1002/adfm.202005201 (2020).
- [30] M. Hayashi, J. Kim, M. Yamanouchi, and H. Ohno, Quantitative characterization of the spin-orbit torque using harmonic Hall voltage measurements, *Phys. Rev. B* 89, 144425 (2014).
- [31] J. Torrejon, J. Kim, J. Sinha, S. Mitani, M. Hayashi, M. Yamanouchi, H. Ohno, Interface control of the magnetic chirality in CoFeB/MgO heterostructures with heavy-metal underlayers, *Nat. Commun.* 5, 4655 (2014).
- [32] C. O. Avci *et al.*, Interplay of spin-orbit torque and thermoelectric effects in ferromagnet/normal-metal bilayers, *Phys. Rev. B* 90, 224427 (2014).
- [33] P. Bruno, Tight-binding approach to the orbital magnetic moment and magnetocrystalline anisotropy of transition-metal monolayers, *Phys. Rev. B* 39, 865 (1989).
- [34] D. Weller, J. Stohr, R. Nakajima, A. Carl, M. G. Samant, C. Chappert, R. Megy, P. Beauvillain, P. Veillet, and G. A. Held, Microscopic Origin of Magnetic Anisotropy in Au/Co/Au Probed with X-Ray Magnetic Circular Dichroism, *Phys. Rev. Lett.* 75, 3752 (1995).
- [35] N. Nakajima, T. Koide, T. Shidara, H. Miyauchi, H. Fukutani, A. Fujimori, K. Iio, T. Katayama, M. Nyvlt, and Y. Suzuki, Perpendicular Magnetic Anisotropy Caused by Interfacial Hybridization via Enhanced Orbital Moment in Co/Pt Multilayers: Magnetic Circular X-Ray Dichroism Study, *Phys. Rev. Lett.* 81, 5229 (1998).
- [36] C. Nistor, T. Balashov, J. J. Kavich, A. Lodi Rizzini, B. Ballesteros, G. Gaudin, S. Auffret, B. Rodmacq, S. S. Dhesi, and P. Gambardella, Orbital moment anisotropy of Pt/Co/AlO<sub>x</sub> heterostructures with strong Rashba interaction, *Phys. Rev. B* 84, 054464 (2011).
- [37] L. Zhu, D. C. Ralph, R. A. Buhrman, Effective Spin-Mixing Conductance of Heavy-Metal-Ferromagnet Interfaces, *Phys. Rev. Lett.* 123, 057203 (2019).
- [38] M.-H. Nguyen, D. C. Ralph, R. A. Buhrman, Spin torque study of the spin Hall conductivity and spin diffusion length in platinum thin films with varying resistivity, *Phys. Rev. Lett.* 116, 126601(2016).
- [39] L. J. Zhu, K. Sobotkiewicz, X. Ma, X. Li, D. C. Ralph, R. A. Buhrman, Strong Damping-Like Spin-Orbit Torque and Tunable Dzyaloshinskii-Moriya Interaction Generated by Low-Resistivity Pd<sub>1-x</sub>Pt<sub>x</sub> Alloys, *Adv. Funct. Mater.* 29, 1805822 (2019).
- [40] X. Wang, A. Manchon, Diffusive Spin Dynamics in Ferromagnetic Thin Films with a Rashba Interaction, *Phys. Rev. Lett.* 108, 117201 (2012).
- [41] A. Manchon and S. Zhang, Theory of spin torque due to spin-orbit coupling, *Phys. Rev. B* 79, 094422 (2009).
- [42] P. M. Haney, H.-W. Lee, K.-J. Lee, A. Manchon, and M. D. Stiles, Current induced torques and interfacial spin-orbit coupling: Semiclassical modeling, *Phys. Rev. B* 87, 174411 (2013).
- [43] P. M. Haney, H. W. Lee, K. J. Lee, A. Manchon, and M.D. Stiles, Current-induced torques and interfacial spin-orbit coupling, *Phys. Rev. B* 88, 214417 (2013).
- [44] L. Zhu, X. Ma, X. Li, R. A. Buhrman, Interfacial Dzyaloshinskii-Moriya interaction and spin-orbit torque in Au<sub>1-x</sub>Pt<sub>x</sub>/Co bilayers with varying interfacial spin-orbit coupling, arXiv:2007.09817 (2020).

## Supplementary Materials for

### Absence of spin current generation in Ti/FeCoB bilayers with strong interfacial spin-orbit coupling

Lijun Zhu\*, Robert A. Buhrman

Cornell University, Ithaca, New York 14850, USA

\*[lz442@cornell.edu](mailto:lz442@cornell.edu)

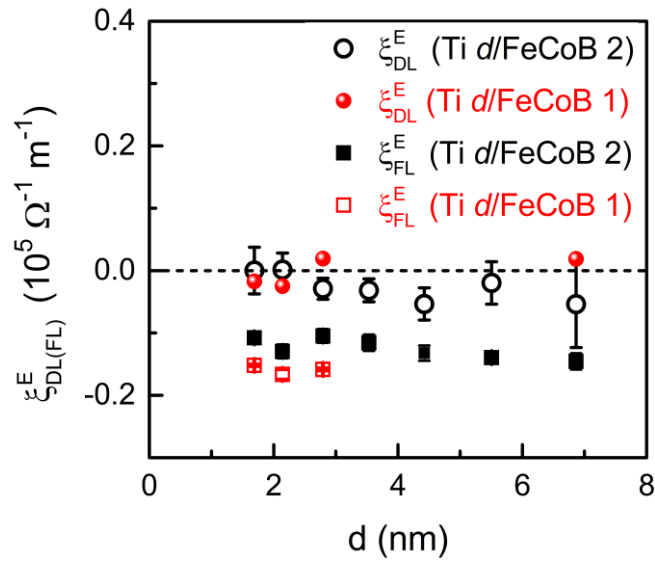


Fig. S1. Dampinglike and fieldlike spin-orbit torques per applied electric field for Ti  $d$ /FeCoB 1 and Ti  $d$ /FeCoB 2.